UNIVERSIDADE DE SÃO PAULO

INSTITUTO DE FÍSICA
CAIXA POSTAL 66318
05315-970 SÃO PAULO - SP
BRASIL

PUBLICAÇÕES

IFUSP/P-1253

STRANGENESS PRODUCTION IN THE MESON CLOUD MODEL

F.S. Navarra, M. Nielsen
Instituto de Física, Universidade de São Paulo

S. Paiva
Instituto de Física Teórica, UNESP
Rua Pamplona 145, 01405-901 São Paulo, SP, Brazil

Dezembro/1996

Strangeness Production in the Meson Cloud Model

F.S. Navarra[1*], M. Nielsen[1†], S. Paiva[2‡]

[1]*Instituto de Física, Universidade de São Paulo*

C.P. 66318, 05389-970 São Paulo, SP, Brazil

[2]Instituto de Física Teórica, UNESP

Rua Pamplona 145, 01405-901 São Paulo, SP, Brazil

Abstract

We have applied the Meson Cloud Model (MCM) to calculate the momentum distribution of kaons and Λ's produced in high energy proton-proton collisions. We show that it is possible ,with no free parameter, to obtain an adequate description of data, especially the large x_F ($x_F \geq 0.2$) part of the spectrum. As expected we underpredict the low x_F part of the curves, where central production mechanisms (fireballs, strings, etc.) are expected to play an important role.

PACS numbers 14.20.Dh 12.40.-y 14.65.-q

---

*e-mail: navarra@if.usp.br

†e-mail: mnielsen@if.usp.br

‡e-mail: samya@if.usp.br

Recent experiments on deep inelastic scattering have renewed the interest on the meson cloud picture of the nucleon. The polarized DIS experiments performed by EMC and SMC collaborations at CERN have shown that only a small fraction of the proton spin is carried by valence quarks. In addition, the strong violation of the Gottfried sum rule observed by NMC strongly suggests a $\overline{d} - \overline{u}$ asymmetry of the nucleon sea. The new fits of the parton distributions to deep inelastic and Drell-Yan data (including the NA51 experiment) seem to confirm the asymmetry. Both the violation of the Gottfried sum rule and the asymmetry measured in Drell-Yan processes can be naturally accounted for by the presence of pions in the nucleon. In view of these successes of the meson cloud model, it is interesting to consider its role in other phenomena. In ref. [1] the MCM has been applied to study rapidity gap events at HERA. The motivation is that rapidity gaps in the observed produced particles require the exchange of a color singlet object, which might be a Pomeron or a meson (most likely a pion). Eventually in a near future this may be clarified with the help of the neutron calorimeter presently under construction.

The meson cloud idea can be applied also to the strange sector. The generalization of the Sullivan [2] process to strange mesons was used in refs. [3,4] to calculate the strange and anti-strange sea quark distributions in the nucleon.

In ref. [5] it is shown that, in contrast to the meson cloud approach expectation, the sea strange and anti-strange quark distributions are quite similar. At first sight this would be a very strong argument against the relevance of the meson cloud [6]. The attempt to explain experimental data with the meson cloud model performed in refs. [3,4] has shown not only that the asymmetry present in this model seems to be in conflict with data but also that the calculated distributions are far below data for $x < 0.3$. However, in ref. [7], these data were reconsidered and combined with the CTEQ collaboration analysis [8]. The conclusion of the authors was that, considering the error bars, existing data do not exclude some asymmetry between the strange and anti-strange momentum distributions, which is significant only for $x > 0.2 - 0.3$. The MCM was also used to estimate the strange radius and strange form factors of the nucleon [9].

In the present work we apply the meson cloud model to analyze strangeness production data. More specifically we address the x_F distributions of K's and Λ's produced in $p-p$ collisions at $p_{lab} \simeq 200 - 400$ GeV/c. These data can be understood in string models in different formulations [10,11]. However, if the meson cloud is responsable for rapidity gap events at HERA, which represent a fraction of $\simeq 10\%$ of all events, it must be important in other experiments as well and, in particular, it must, at least partially, explain strangeness production at mid and large rapidities. In the case of the strange meson cloud, the cloud parameters (cut-off and coupling constant) are known from other type of experiments and a parameter free calculation is possible. An additional reason for using the MCM to study strangeness production is that string models (see in this particular point ref. [10]) seem to give strange particle spectra with a too strong energy dependence, not observed in experimental data. The meson cloud model, on the other hand, in its usual version, has no energy ($\sqrt{s}$) dependence.

In the picture adopted here, in a sizeable fraction of the events the Λ and K already preexist as a virtual state in the projectile carrying nucleon fractional momenta y_Λ and y_K respectively, which follow the meson cloud model distribution $f_K(y)$ given by [4,12]

$$f_K(y) = \frac{g^2_{KN\Lambda}}{16\pi^2}\, y \int_{-\infty}^{t_{max}} dt\, \frac{[-t + (m_\Lambda - m_N)^2]}{[t - m_K^2]^2}\, F^2(t)\,, \tag{1}$$

where $t = k^2$ is the meson virtuality. In the above expression $F(t)$ is a form-factor at the $KN\Lambda$ vertex, and t_{max} is the maximum value of k^2, determined purely by kinematics:

$$t_{max} = m_N^2 y - \frac{m_\Lambda^2 y}{1-y}\,. \tag{2}$$

For the $KN\Lambda$ form factor, following a phenomenological approach, we use the exponential form:

$$F_{KN\Lambda}(t) = e^{(t-m_K^2)/\Lambda^2_{KN\Lambda}}\,, \tag{3}$$

In the above expressions m_N, m_Λ and m_K are the nucleon mass, the mass of the intermediate Λ and the K meson mass respectively. $\Lambda_{KN\Lambda}$ is the form factor cut-off parameter.

In the MCM there are two parameters involved : the above mentioned cut-off and the nucleon-barion-meson coupling constant $g_{KN\Lambda}$. In contrast to other calculations, we are not interested here in absolute numbers but rather in differential distributions. Since other processes (e.g., central production) are responsable for strangeness production the cloud is meant to explain only the fast part of the spectrum being thus unable to account for the total cross section and for the overall normalization of the spectra. The coupling constant always appears as a multiplicative factor and therefore it is irrelevant in our case. The cut-off $\Lambda_{KN\Lambda}$ is thus the only parameter and is not free because it has been already fixed in other MCM applications to the description of data. In [4] an extensive discussion concerning the appropriate value of the cut-off has been made. In our analysis we use the smallest ($\Lambda_{KN\Lambda} = 750$ MeV) and the largest ($\Lambda_{KN\Lambda} = 1200$ MeV) values compatible with phenomenological and theoretical studies.

The exponential form factor is not the only possible choice. We could use a monopole or even dipole form as well. Differences between the various forms are not particularly important and, besides, as it was pointed out in [4] it is possible to "translate" one form factor with its cut-off to another form factor with a correspondingly different cut-off, the overall results being approximately equivalent. Therefore we restrict ourselves to the exponential form (3).

Since we are addressing low p_T data it is reasonable to think that the projectile is disturbed but not destroyed by the interaction. Through soft interactions it is decelerated keeping a fraction x_L of its original momentum. This interaction is sufficient to put the Λ and the K in the cloud on the mass shell with momenta x_Λ and x_K. It is important to stress that after the interaction we have

$$x_K + x_\Lambda = x_L \tag{4}$$

but the function $f_K(y)$ is not significantly distorted. For small values of x_L (large energy loss of the projectile) this approximation becomes unjustified. A similar approximation has been used in the series of works on intrinsic charm by Vogt and Brodsky [13], where it was

assumed that virtual particles come to mass shell through soft interactions conserving their previous ("intrinsic") momentum distribution.

The kaon momentum distribution is, therefore, given by the simple convolution

$$\frac{dN}{dx_K} = \int_{x_K}^1 \frac{dx_L}{x_L} g(x_L) f_K(\frac{x_K}{x_L}) \tag{5}$$

where the function $g(x_L)$ is the momentum distribution of the outgoing excited proton and may be well approximated by the leading proton spectrum, which, in the energy range considered here, has been measured. We parametrize the data of ref. [14] as

$$\frac{x_L}{\sigma}\frac{d\sigma}{dx_L} = a\, x_L^b + c \tag{6}$$

Since data cover only the range $0.3 \leq x_F \leq 0.88$ several parameter choices are possible. The corresponding spectra will be very different in the unmeasured region. We take two parameter sets: $a = 13.56$, $b = 1$ and $c = 1.51$ (set I) and $a = 11$, $b = 2$ and $c = 5$ (set II). In Fig.1 we show the parametrization (6) with set I (solid line), with set II (dashed line) and data points. There is a significant difference in the low x ($x \leq 0.3$) region. As it will be seen, a higher curve in this region will lead to an enhancement in the strange particle spectrum in the same x region. In our approach this ambiguity is not a major problem since we do not make any attempt to be very precise in this domain, where the cloud picture is not expected to work very well. The inclusion of the leading particle spectrum here is essential in two aspects. In first place without it the K and Λ spectra would be much narrower and too much forward peaked. They would be hopelessly far from experimental points. In second place the l.p. spectrum contains all the energy dependence of the problem. The cloud itself has the same properties for all projectile energies. The leading particle momentum distribution ($g(x_L)$) was never measured at higher energies. Models [15,16] predict a weak energy dependence. This seems to be consistent with the observed energy behaviour of the strange particle spectra.

The x_Λ distribution is obtained with the assumption [3] that the amplitude to find an intermediate baryon with momentum fraction y in the nucleon is the same as to find an intermediate meson with momentum fraction $(1-y)$ in the nucleon. We have then

$$\frac{dN}{dx_\Lambda} = \int_{x_\Lambda}^{1} \frac{dx_L}{x_L} g(x_L) f_K(1 - \frac{x_\Lambda}{x_L}) \qquad (7)$$

Since we are interested in inclusive production of K's we should in principle include other types of clouds and specially the $K\,\Sigma$ and $K\,\Sigma^*$ fluctuations of the nucleon. Eq. (1) would then contain a sum over all these virtual states as in most of the works [4] with the MCM. States containing Σ are more massive than those containing Λ. Moreover, according to phenomenological estimates [17] the coupling constant $g_{KN\Sigma}$ (= 2.69) is very small compared to $g_{KN\Lambda}$ (= 13.98). We therefore do not expect them to be important here. However the coupling $g_{KN\Sigma^*}$ (= 14.3) is very large [4] and in ref. [12] it has been shown that the $K\Sigma^*$ state gives a non negligible contribution to the $\overline{s}$ distribution in the nucleon. A numerical computation of the function $f_K(y)$ for the $K\Sigma^*$ [4,12] case shows that the result is very similar in shape to the result of eq. (1). The Σ^* seems to play a role in the constitution of the strange sea of the nucleon but on the other hand the experimentally measured cross section for Σ^* production [18] is much smaller than the cross section for Λ production [19]. This indicates that the kaons produced in association with the Σ^*'s are much less abundant than those produced in association with the Λ's. Considering what was said above we conclude that the $K\Sigma^*$ state is much more difficult to put on the mass shell and gives a small contribution to the total kaon yeld. We shall therefore assume that the kaons coming from these states are, if present, well represented by the kaon distribution of the $KN\Lambda$ cloud. Another aspect of inclusive K production is resonance formation and decay. It has been reported [20] that a significant fraction of the measured K's comes from the resonance K^*, which decays mostly through the channel $K^{*\pm} \rightarrow K^0\pi^\pm$. In addition to direct K production we should thus include a contribution coming from the ΛK^* state (we neglect $\Sigma^* K^*$ because of its larger mass and smaller cross section). A numerical comparison between $f_K(y)$ and $f_{K^*}(y)$ [21] shows that the difference between them is small, the K^*'s being slightly faster than the K's. During its conversion into a K^0, the K^* emitts a pion and becomes softer. At a qualitative level one effect compensates the other. A more quantitative analysis requires some modelling of the K^* decay. We prefer, in a first approximation, to

consider the indirect K spectrum equal to the direct one.

Before making comparison with experimental data some remarks are in order. Leading particle spectra in ref. [14] are measured at $p_T = 0.3$ GeV/c, data of refs. [19,20,22,23] are integrated over p_T and our version of the meson cloud model is one dimensional. Because of this reason some discrepancy is expected in the low x region, where p_T can be large. In the forward region p_T has to be small and a one dimensional treatment is reasonable. Moreover, some experimental papers on strangeness production present $d\sigma/dx$ and some others present the invariant cross section integrated over p_T. This last quantity differs from $xd\sigma/dx$ (which we can compute in our model) by a constant factor only for $x \geq 0.3$. For smaller values of x their difference is x dependent and our calculations become less reliable.

Having these restrictions in mind we can compare eqs. (5) and (7) (which are in arbitrary units) directly with data. In Fig. 2a we compare the MCM prediction for the kaon spectrum with the data of ref. [22] (black circles) and ref. [20] (squares). The lines show the meson cloud model results with two values of the cut-off : $\Lambda = 0.75$ GeV (dashed line) and $\Lambda = 1.2$ GeV (solid line). Distribution (6) was used with set I of parameters. The only arbitrary parameter is the normalization constant and it is properly chosen to give a good description of data at large x, where the cloud picture is supposed to work better. As expected, we obtain a reasonable agreement with data at large x and underpredict them at low x. In this region, central production is probably dominant. Fig. 2b shows the same as 2a but the (6) was calculated with parameter set II. As it can be seen, using set II produces an enhancement in the low x part of the curves and has no effect on the large x tail. Fig. 3a shows our prediction for the Λ spectrum (with set I in (6)) and compare it with those measured in [22] (black circles) and [20] (squares). A similar behaviour is observed but the general agreement is better. This is not surprising. Because of their larger mass its more difficult to produce Λ's than K's in the central region and therefore the K "excess" with respect to our predictions is more pronounced than the Λ "excess". Fig. 3b shows the effect of replacing set I by set II in the distribution (6). Again we see that (7) is quite stable under changes in the parameters of (6). Fig. 4 shows the Λ spectrum measured in [19] and our

results. In Fig. 5a and 5b we show combined data of refs. [20] and [23] on the invariant cross section as a function of x for K's and Λ's respectively. Once again the same behaviour is observed.

In all the curves presented the integrated MCM distributions will give the cross section of producing K's or Λ's through the cloud mechanism to be compared with the corresponding total strange particle production cross sections. Neglecting the weak energy dependence, the MCM K and Λ cross sections are about $\simeq 60\%$ and $\simeq 75\%$ of the total cross sections respectively. These numbers must be viewed as upper limits since we have integrated our curves over the very low x region where our model is no longer valid.

As it has been pointed out in the literature [7,24,25] , to a large extent, we can identify the strangeness in the cloud with the "intrinsic strangeness" and identify "centrally produced strangeness" with the "extrinsic strangeness". This allows us to compare our results with the results of the intrinsic charm model for charm production. A systematic study of charm production with a two component model (extrinsic + intrinsic component), completed in ref. [13] arrived at the conclusion that in order to explain the x_F distributions of the produced charmed particles the intrinsic component (or cloud component in our language) must be of $\simeq 20\%$ of the total cross section. Considering that strange fluctuations in the nucleon are much more likely to happen than those with charm quarks and that it is easier to put the former in the mass shell, we conclude that our estimates are compatible with those found in ref. [13].

This work was motivated by the recent revival of the meson cloud picture of the nucleon. The main conclusion of this note is that the MCM describes reasonably well the production of fast strange particles. It starts to fail at $x \simeq 0.2$, precisely the region where it also fails in describing the strange quark distribution in the nucleon, as pointed out in [4].

One of the predictions of the meson cloud model is the existence of an asymmetry between produced strange particles having quarks in common with the nucleon projectile and produced strange particles without them, the latter being less abundant than the former, specially at large x_F. In [26] this effect was experimentally observed for the K^+/K^- ratio.

It would be very interesting to confirm this behaviour in a more sytematic way, as done recently for charm particles.

Acknowledgements: This work has been supported by FAPESP and CNPq.

REFERENCES

[1] M. Przybycien, A. Szczurek and G. Ingelman, DESY Report DESY 96-073 ; hep-ph/9606294.

[2] J.D. Sullivan, *Phys.Rev.* **D5**, 1732 (1972).

[3] A.I. Signal and A.W. Thomas, *Phys. Lett.* **B191**, 205 (1987).

[4] W. Koepf, L.L. Frankfurt and M. Strikman, *Phys.Rev.* **D53**, 2586 (1996).

[5] CCFR Collaboration, A.O. Bazarko et al., *Z. Phys.* **C65**, 189 (1995).

[6] X. Ji and J. Tang, *Phys. Lett.* **B362**, 182 (1995).

[7] S.J. Brodsky and B.Q. Ma, *Phys. Lett.* **B381**, 317 (1996).

[8] CTEQ Collab., J. Botts et al., *Phys. Lett.* **B304**, 159 (1993); W.L. Lai et al., *Phys.Rev.* **D51**, 4763 (1995).

[9] see for example H. Forkel, M. Nielsen, X. Jin and T.D. Cohen, *Phys.Rev.* **C50**, 3108 (1994) and references therein.

[10] K. Werner, *Phys.Rep.* **232**, 87 (1993).

[11] T. Kodama, R. Nazareth, G. Pech, C. Aguiar, *Phys.Rev.* **C56**, 59 (1996).

[12] "Virtual meson cloud of the nucleon and intrinsic strangeness and charm", S. Paiva et al., IFUSP Report IFUSP/P-1240, hep-ph/9610310.

[13] R. Vogt and S.J. Brodsky, *Nucl.Phys.* **B478** (1996) 311 and references therein.

[14] Barton et al., *Phys.Rev.* **D27**, 2580 (1983).

[15] G.N. Fowler et al., *Phys.Rev.* **C41**, 1219 (1989).

[16] Y. Hama and S. Paiva, "Inelasticity distributions in high energy p-nucleus collisions", report IFUSP/P-1243 (1996).

[17] B. Holzenkamp, K. Holinde and J. Speth, *Nucl. Phys.* **A500**, 485 (1989).

[18] F. LoPinto et al., *Phys.Rev.* **D22**, 573 (1980).

[19] S. Erhan et al., *Phys. Lett.* **B85**, 447 (1979).

[20] H. Kichimi et al., *Phys.Rev.* **D20**, 37 (1979).

[21] W.-Y.P. Hwang, J. Speth and G.E. Brown, *Z. Phys.* **A339**, 383 (1991).

[22] K. Jaeger et al., *Phys.Rev.* **D11**, 2045 (1975).

[23] EHS-RCBC Collaboration, M. Asai et al., *Z. Phys.* **C27**, 11 (1985).

[24] F.S. Navarra, M. Nielsen, C.A.A. Nunes and M. Teixeira, *Phys.Rev.* **D54**, 846 (1996) and references therein.

[25] The relation between the meson cloud and intrinsic states was first pointed out in S.J. Brodsky, C. Peterson and N. Sakai, *Phys.Rev.* **D43**, 59 (1991).

[26] J.R. Johnson et al., *Phys.Rev.* **D17**, 1292 (1978)

Figure Captions

Fig. 1 Leading proton spectrum. Points are data from [14]. Solid and dashed lines are the parametrizations I and II respectively.

Fig. 2 a) x_F distribution of kaons calculated with the MCM and compared with data of ref. [22] (circles) and of ref. [20] (squares). Eq. (6) was calculated with set I of parameters; b) the same as a) with set II. Solid and dashed lines are for Λ equal to 1.2 GeV and 0.75 respectively.

Fig. 3 a) Λ spectrum calculated with the MCM and compared with data of ref. [22] (circles) and of ref. [20] (squares). Eq. (6) was calculated with set I of parameters; b) the same as a) for set II. Solid and dashed lines are for Λ equal to 1.2 GeV and 0.75 respectively.

Fig. 4 Λ spectrum measured in ref. [19] (points) and MCM calculation (solid line).

Fig. 5 a) Invariant cross section as a function of x for kaons(points) and MCM calculation (lines); b) the same as a) for Λ's. Data are from ref. [23] (circles) and [20] (squares) .

Figure 1

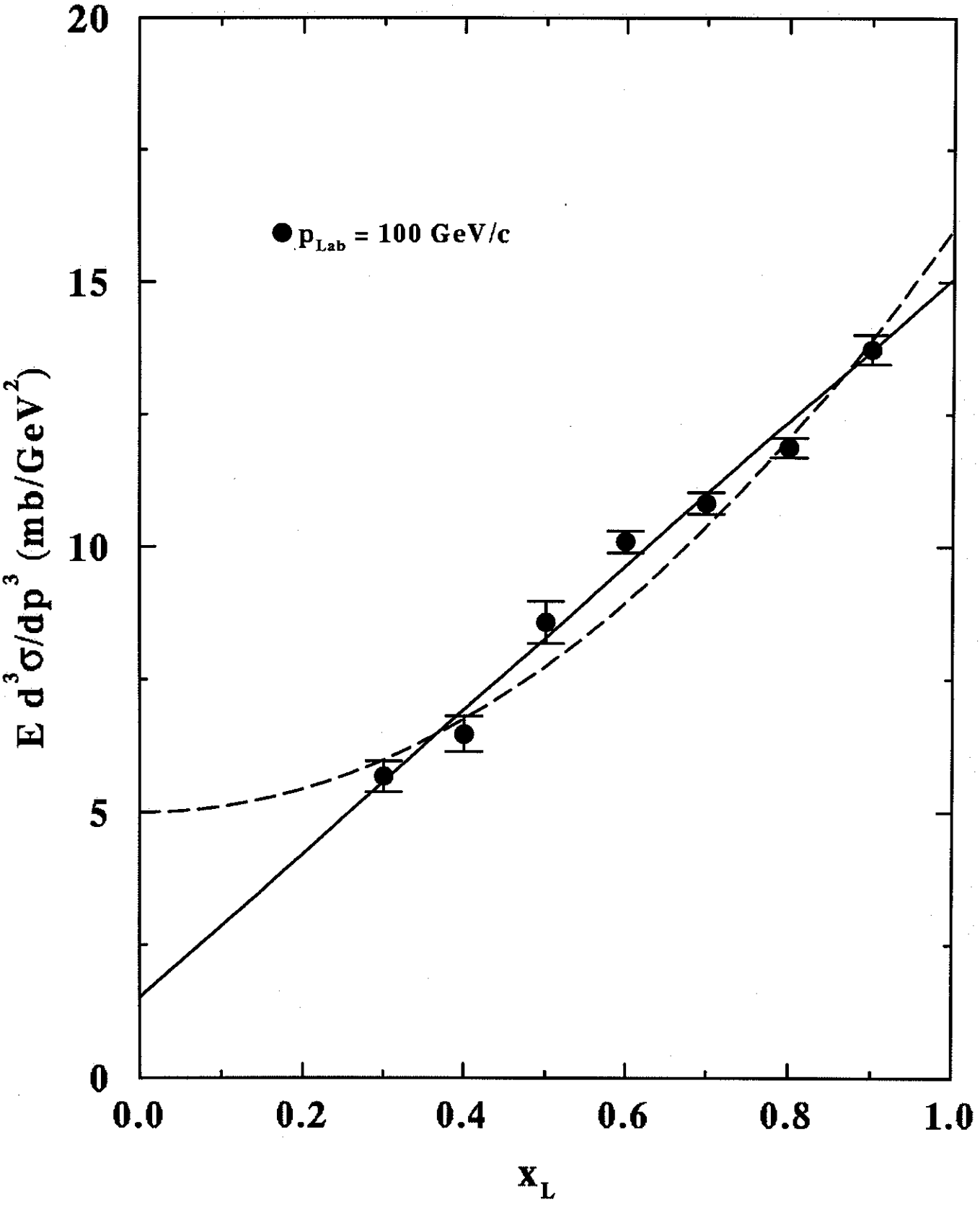
20
15
10
5
0
0.0
0.2
0.4
0.6
0.8
1.0
$E\,d^3\sigma/dp^3$ (mb/GeV^2)
x_L
p_{Lab} = 100 GeV/c

Figure 2a

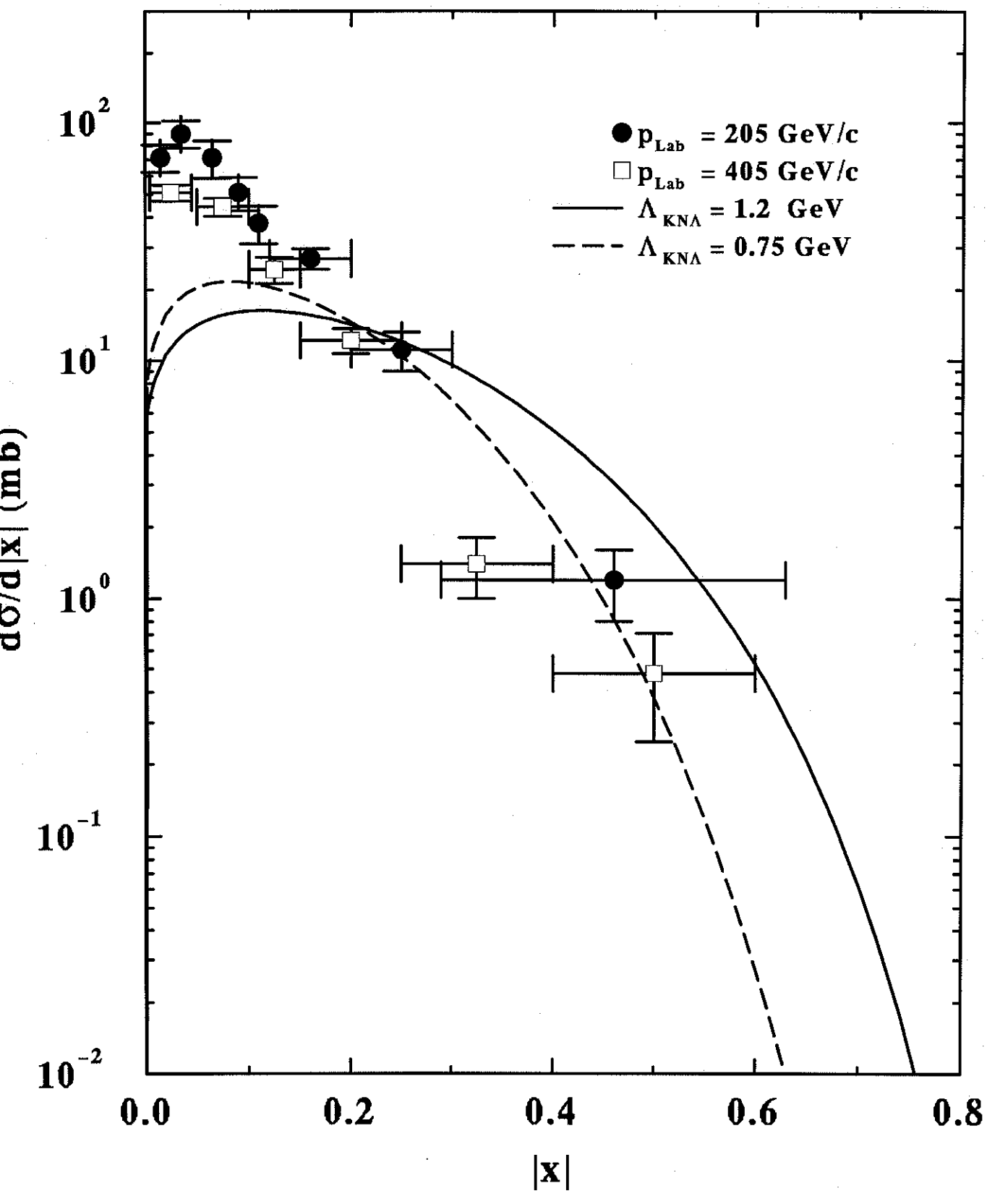
10^2
10^1
10^0
10^{-1}
10^{-2}
$d\sigma/d|x|$ (mb)
0.0
0.2
0.4
0.6
0.8
|x|
p_{Lab} = 205 GeV/c
p_{Lab} = 405 GeV/c
$\Lambda_{KN\Lambda}$ = 1.2 GeV
$\Lambda_{KN\Lambda}$ = 0.75 GeV

Figure 2b

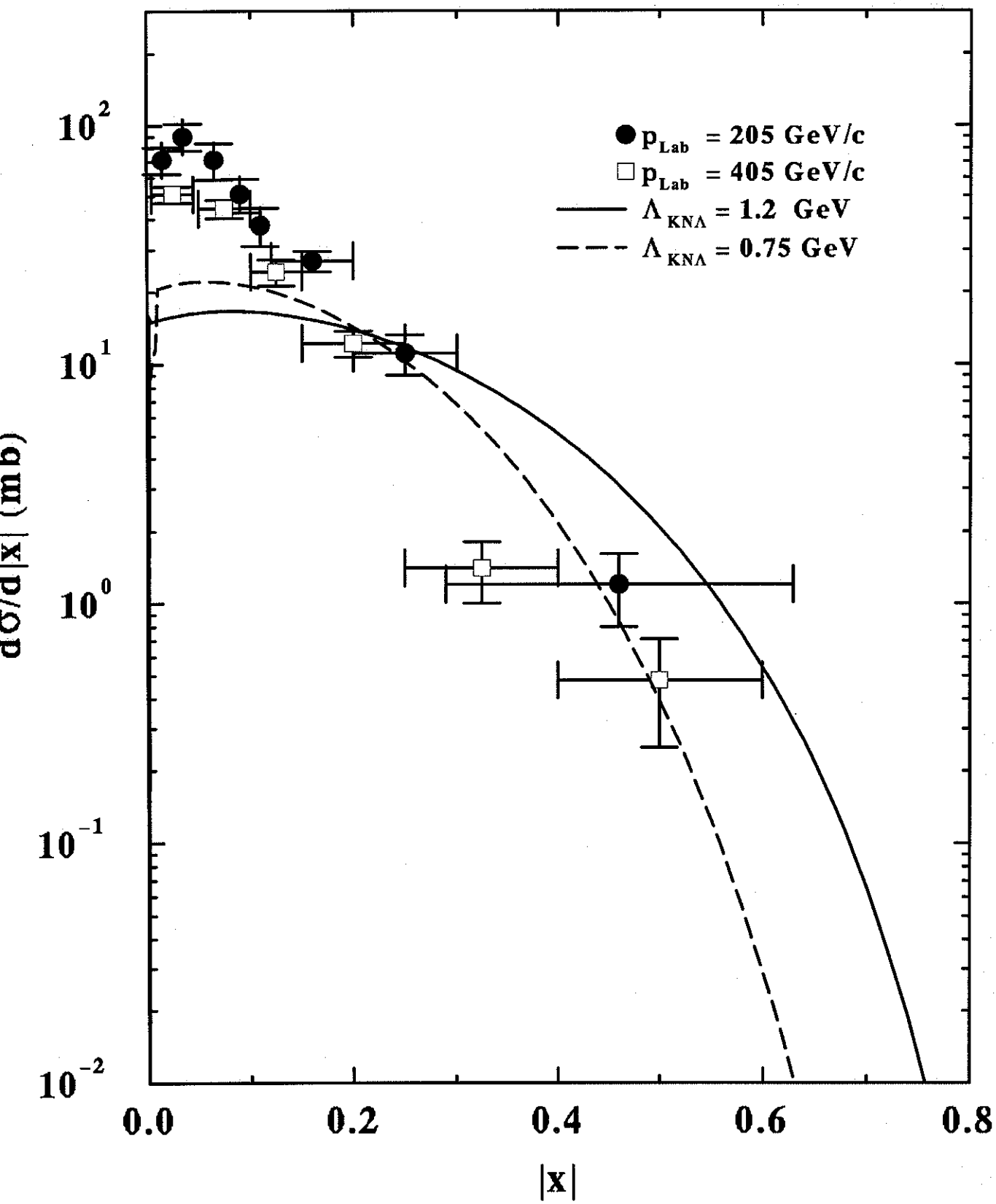
10^2
10^1
10^0
10^{-1}
10^{-2}
$d\sigma/d|x|$ (mb)
0.0
0.2
0.4
0.6
0.8
|x|
p_{Lab} = 205 GeV/c
p_{Lab} = 405 GeV/c
$\Lambda_{KN\Lambda}$ = 1.2 GeV
$\Lambda_{KN\Lambda}$ = 0.75 GeV

Figure 3a

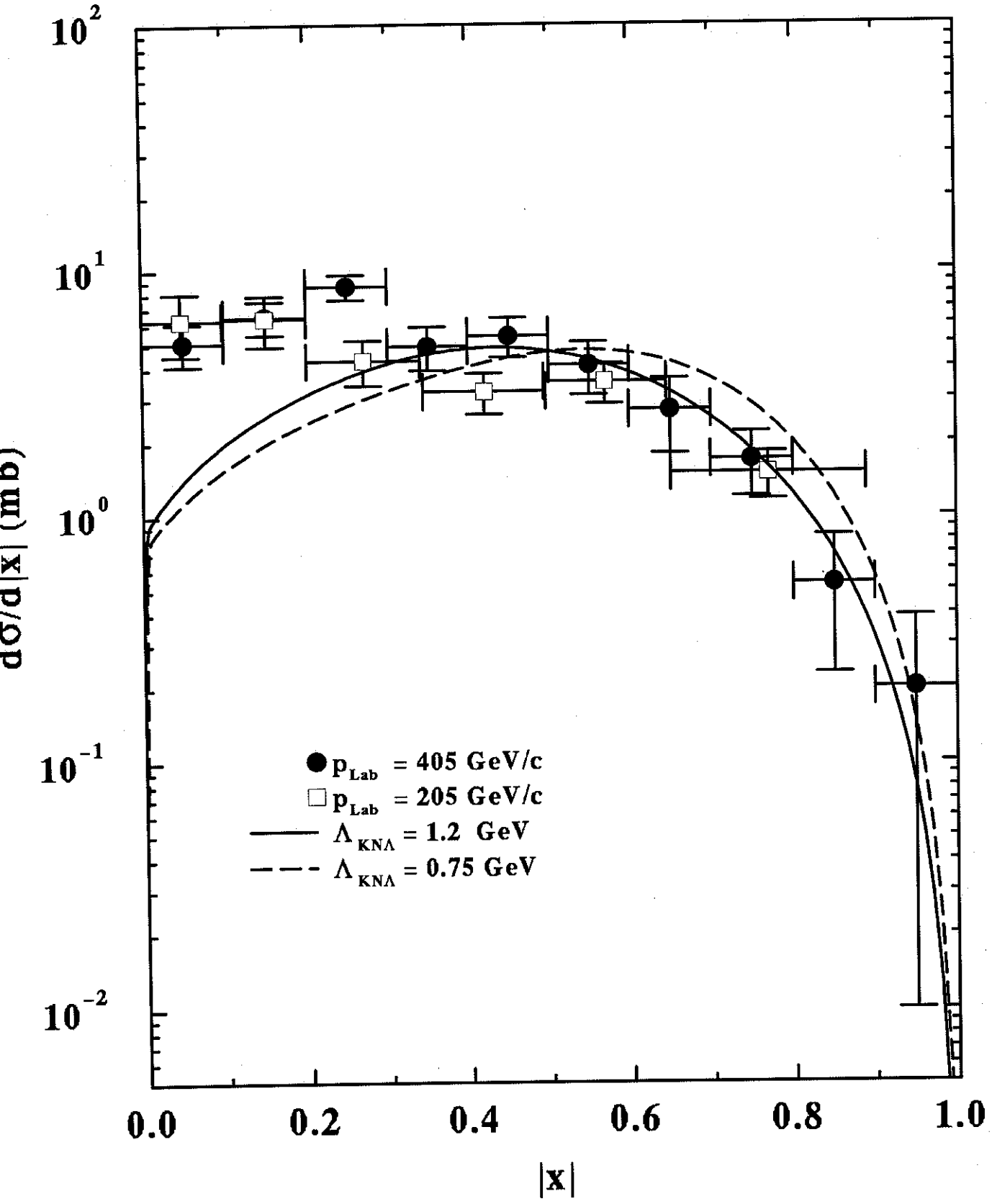
10^2
10^1
10^0
10^{-1}
10^{-2}
$d\sigma/d|x|$ (mb)
p_{Lab} = 405 GeV/c
p_{Lab} = 205 GeV/c
$\Lambda_{KN\Lambda}$ = 1.2 GeV
$\Lambda_{KN\Lambda}$ = 0.75 GeV
0.0
0.2
0.4
0.6
0.8
1.0
|x|

Figure 3b

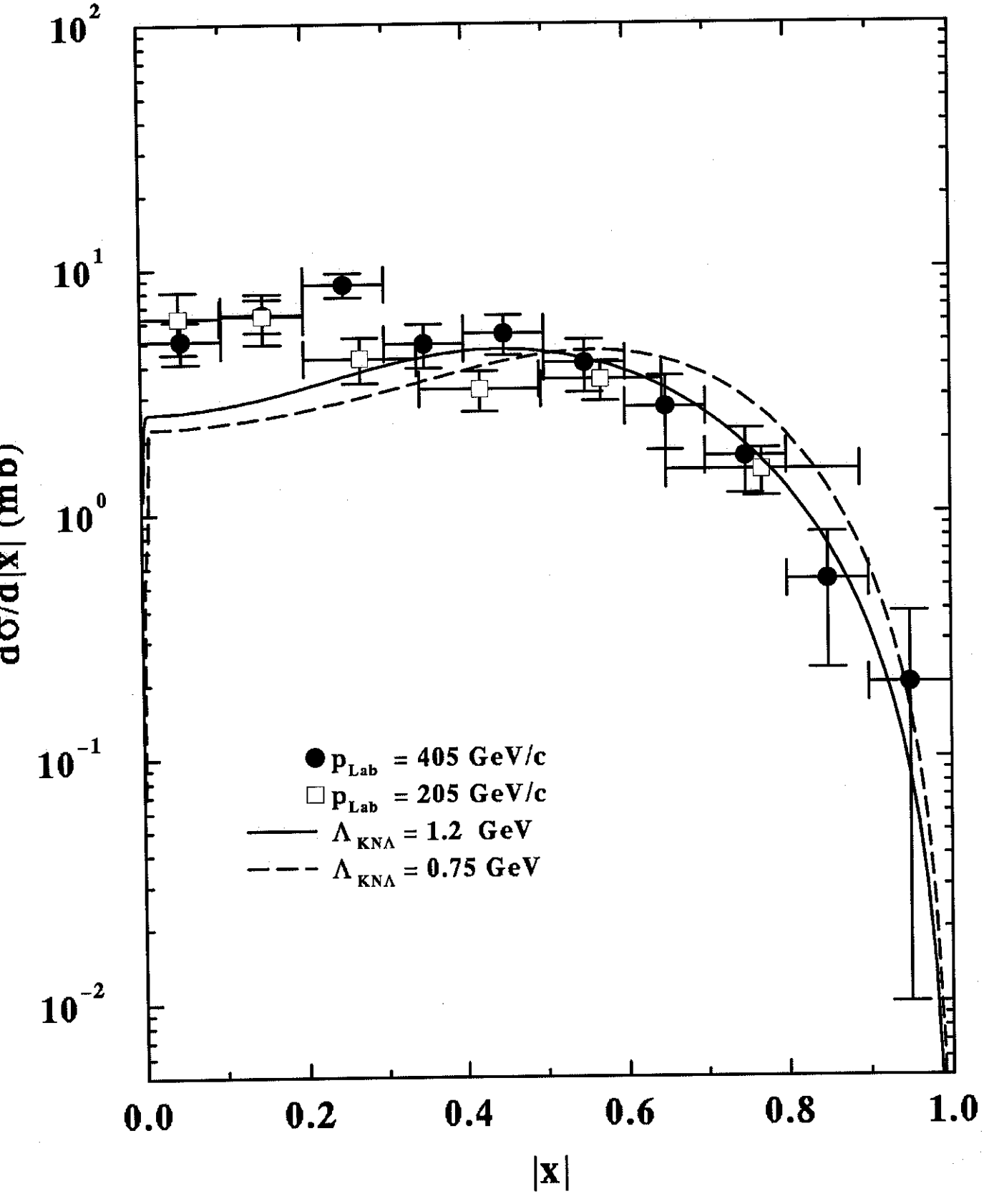
10^2
10^1
10^0
10^{-1}
10^{-2}
dσ/d|x| (mb)
● p_{Lab} = 405 GeV/c
□ p_{Lab} = 205 GeV/c
$\Lambda_{KN\Lambda}$ = 1.2 GeV
$\Lambda_{KN\Lambda}$ = 0.75 GeV
0.0
0.2
0.4
0.6
0.8
1.0
|x|

Figure 4

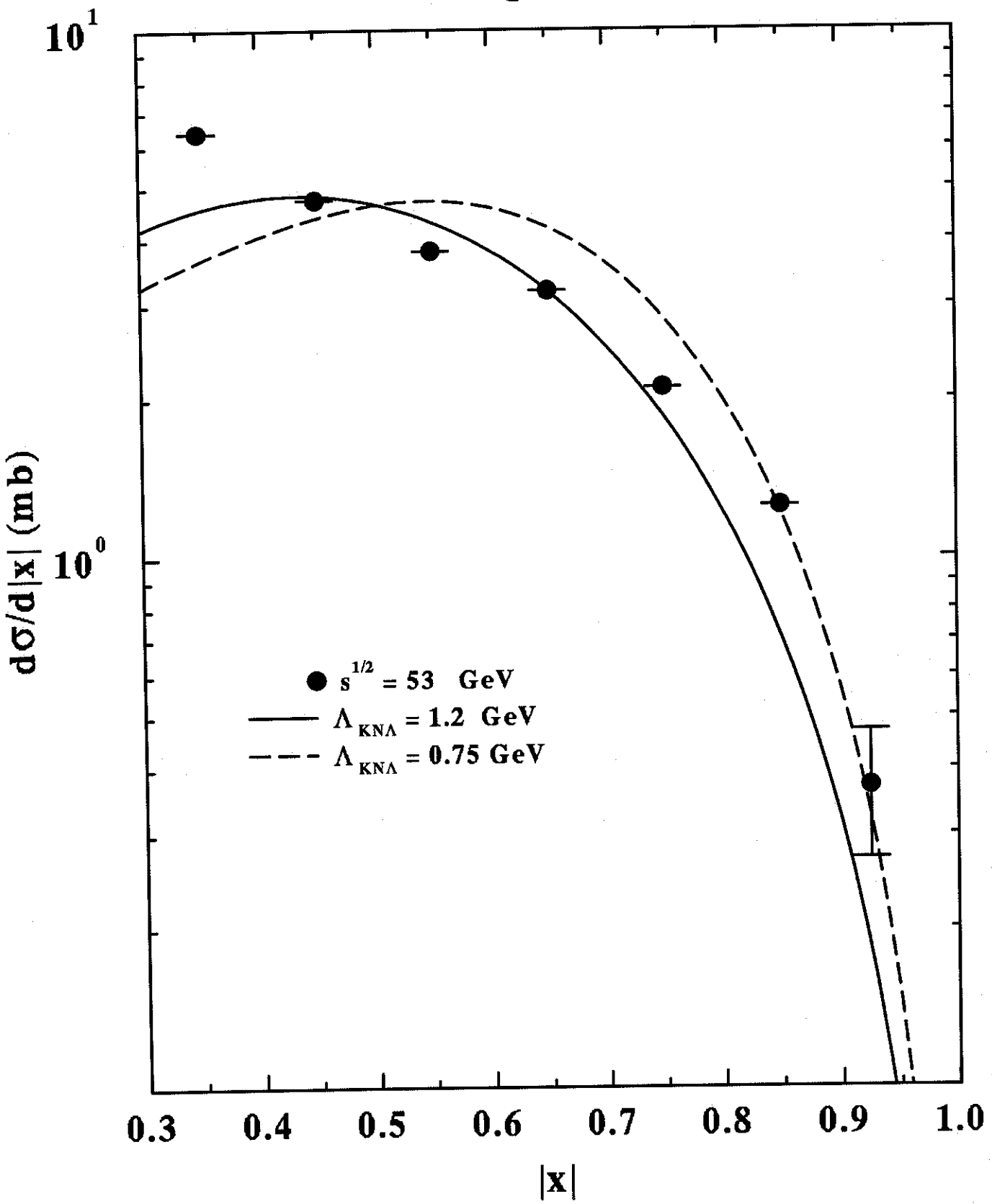
10^1
10^0
$d\sigma/d|x|$ (mb)
$s^{1/2}$ = 53 GeV
$\Lambda_{KN\Lambda}$ = 1.2 GeV
$\Lambda_{KN\Lambda}$ = 0.75 GeV
0.3
0.4
0.5
0.6
0.7
0.8
0.9
1.0
|x|

Figure 5a

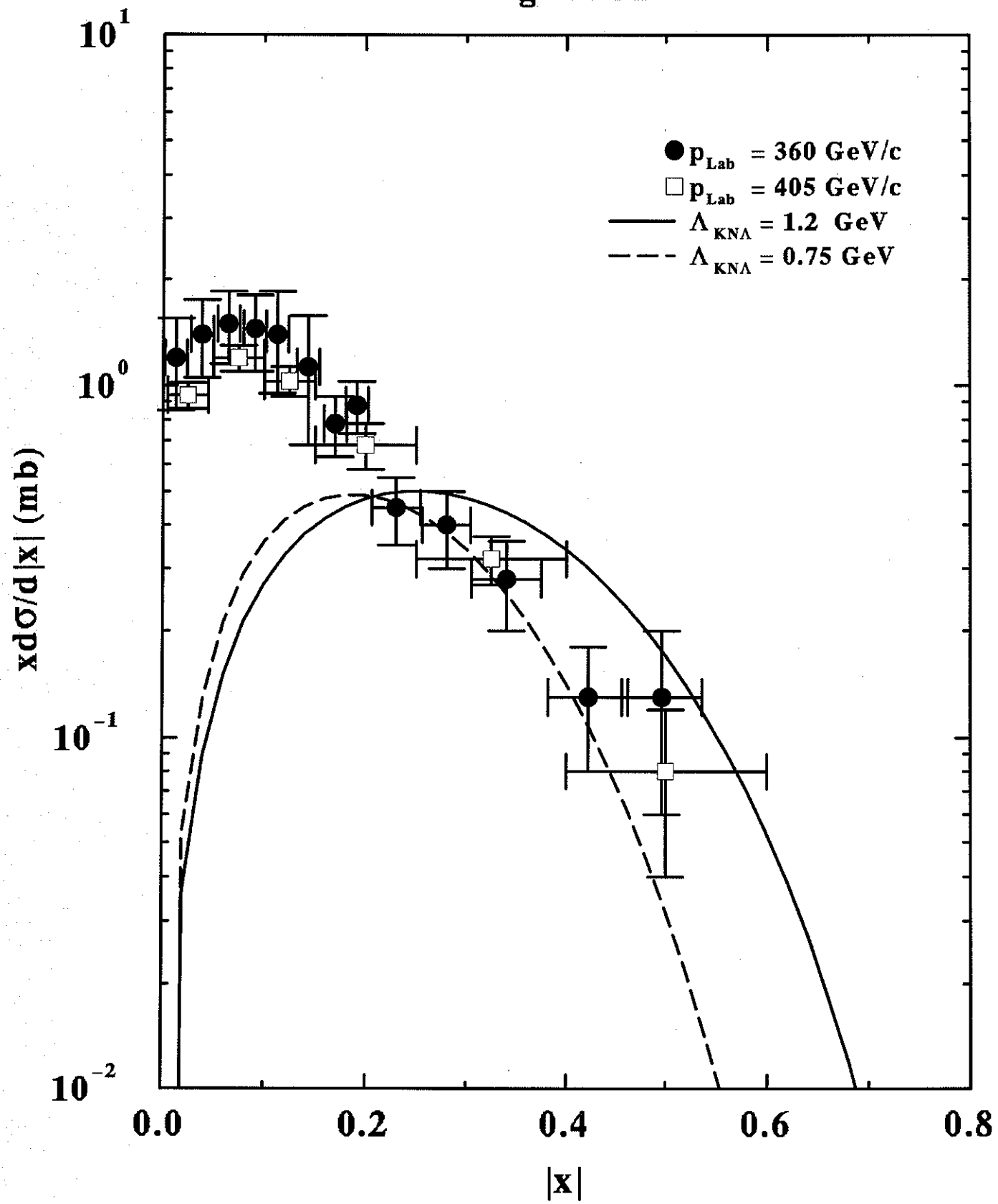
10^1
10^0
10^{-1}
10^{-2}
$x d\sigma/d|x|$ (mb)
0.0
0.2
0.4
0.6
0.8
|x|
p_{Lab} = 360 GeV/c
p_{Lab} = 405 GeV/c
$\Lambda_{KN\Lambda}$ = 1.2 GeV
$\Lambda_{KN\Lambda}$ = 0.75 GeV

Figure 5b

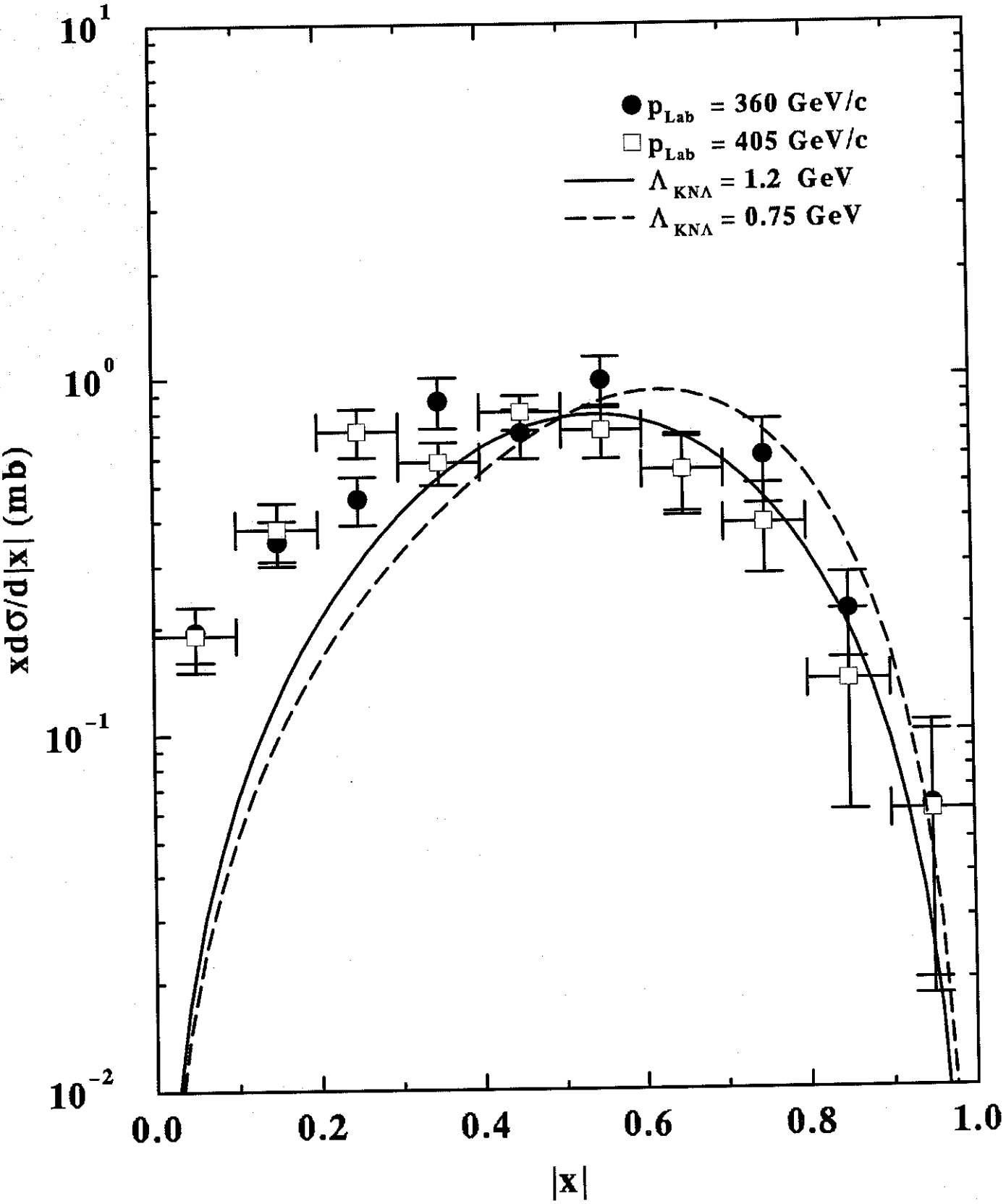
10^1
10^0
10^{-1}
10^{-2}
$x d\sigma/d|x|$ (mb)
● p_{Lab} = 360 GeV/c
□ p_{Lab} = 405 GeV/c
$\Lambda_{KN\Lambda}$ = 1.2 GeV
$\Lambda_{KN\Lambda}$ = 0.75 GeV
0.0
0.2
0.4
0.6
0.8
1.0
|x|